Konrad-Zuse-Zentrum
für Informationstechnik Berlin

Takustraße 7
D-14195 Berlin-Dahlem
Germany

HEIKO SCHMIDT[1] CARMEN JIMÉNEZ[2]

Numerical study of the direct pressure effect of acoustic waves in planar premixed flames[3]

[1]Zuse Institute Berlin (ZIB),
e-mail: heischmi@math.fu-berlin.de
[2]Centro de Investigaciones Energéticas, Medioambientales y Tecnologicas, Avenida Complutense, 22, 28040, Madrid, Spain,
e-mail: carmen.jimenez@ciemat.es
[3]submitted to Combustion and Flame

This work was partially supported by the Spanish Ministry of Science through project ENE-2008-06515-C04-02 and Madrid's Regional Government through the COMLIMAMS program.

ZIB-Report 09-31 (October 2009)

Numerical study of the direct pressure effect of acoustic waves in planar premixed flames

H. Schmidt, C. Jiménez

October 16, 2009

Abstract

Recently the unsteady response of 1-D premixed flames to acoustic pressure waves for the range of frequencies below and above the inverse of the flame transit time was investigated experimentally using OH chemiluminescence [22]. They compared the frequency dependence of the measured response to the prediction of an analytical model proposed by Clavin et al. [2], derived from the standard flame model (one-step Arrhenius kinetics). Discrepancies between the experimental results and the model led to the conclusion that the standard model does not provide an adequate description of the unsteady response of real flames and that it is necessary to investigate more realistic chemical models. Here we follow exactly this suggestion and perform numerical studies of the reponse of lean methane flames using different reaction mechanisms. We find that the global flame response obtained with both detailed chemistry (GRI3.0 [21]) and a reduced multi-step model by Peters [17] lies slightly above the predictions of the analytical model, but is close to experimental results. We additionally used an irreversible one-step reaction model which yields good results at least for frequencies close to the inverse flame transit time.

Keywords: Direct pressure effect, acoustics, flame response

Contents

1 Introduction

Thermoacoustic instabilities in a combustion chamber can be seen as self-sustained pressure fluctuations under an unsteady combustion process. The phenomenon is still a subject of intensive research, because it negatively affects the structure of the chamber and the efficiency of the combustion process. Combustion instability involves a complex dynamical interaction between unsteady heat release, acoustic fluctuations, and the flow. The latter influence on the instability mechanism is e.g. investigated in [19], [24], and [20]. The modulation of the inlet feeding rate via sound waves, producing changes in equivalence ratio of the burning mixture was investigated among other in [11], [15], and [14]. Sound can also affect the flame surface area as e.g. shown in [4] or [3]. Perhaps the most intuitive, but yet not fully understood, interaction is the **direct pressure effect**, that is, the direct impact of acoustic pressure fluctuations on the chemical reaction rates, see e.g. [23]. This latter effect can be isolated by restricting the study to one dimensional, planar, premixed flames.

In the paper we numerically investigate the unsteady response of 1-D premixed planar lean methane flames to acoustic pressure waves for the range of frequencies below and above the inverse of the flame transit time and compare the results to recent experiments [22].

We use two totally different numerical codes and vary as well the complexity of the methane reaction mechanism. The paper is organized as follows: In the next section we summarize the relevant theoretical results for the direct pressure effect which we use for comparison with our numerical data. In section 3 we summarize our numerical model. Section 4 shows the results obtained with the compressible and incompressible ansatz for different chemistry models and compares them to the experiments and theory. Finally, we finish with some concluding remarks.

2 Background

The direct effect of an oscillating pressure on a planar flame has been described analytically by Clavin et al. [2] and McIntosh [12, 13], based on a formulation of the standard flame model with one step chemistry governed by an Arrhenius law.

Fig. 1 presents a sketch of the studied problem: an acoustic wave of amplitude p' and wavelength λ propagating at the speed of sound c incides on a planar premixed flame with width δ_f and flame speed s_l. The characteristic times associated to the wave and the flame are $\tau = 1/\omega = \lambda/c$ and $\tau_f = \delta_f/s_l$, respectively, and the flame Mach number, $Ma = s_l/c$ is much smaller than one.

Clavin et al. study the effect of waves of small amplitude p' and moderate frequency, that is, with ω of the order of the inverse of the flame transit time. This corresponds to $\omega\tau_f = \tau_f/\tau = O(1)$, and thus to wavelengths much longer than the flame thickness: $\frac{\delta_f/s_l}{\lambda/c} = O(1) \Rightarrow \lambda = \delta_f/Ma >> \delta_f$, if we restrict ourselves to flame speeds slow compared to the speed of sound. Thus in the studied problem acoustic waves are seen by the flame as pulses of time–varying pressure, uniform across the flame width, and no spatial pressure variation can be seen by the flame.

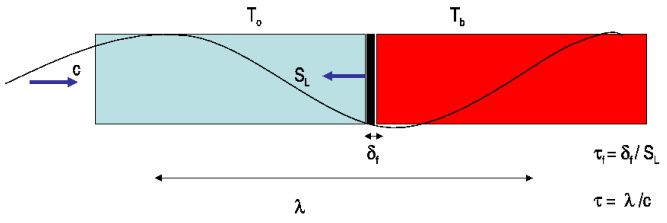

Figure 1: Sketch of the studied problem: an acoustic wave propagating towards a planar premixed flame

Clavin et al. [2] predict fluctuations for the mass flux $\dot{m}'$,

$$\frac{\dot{m}'/\rho s_l}{p'/\rho c^2} = \frac{Ea}{RTb}\left(\gamma - 1\right)\frac{A(\omega)}{B(\omega)} i\omega\tau_f \tag{1}$$

with

$$\begin{aligned} A(\omega) &= \left(q - \left(T_b - T_0\right)/T_b\right) q \\ B(\omega) &= \left(q-1\right) q^2 - \frac{\beta}{2}\left(Le - 1\right)\left(1 - q + 2i\omega\tau_f\right) \\ q(\omega) &= \left(1 + 4i\omega\tau_f\right)^{\frac{1}{2}}. \end{aligned}$$

This mass flux is not a directly measurable quantity, given that for non stationary flames it is not equivalent to the mass consumption rate, as is the case in steady planar flames.

The model for $\dot{m}'$ can be used to derive a model for fluctuations in the heat release rate $\dot{Q}'$ [22, 2]:

$$\frac{\dot{Q}'/\overline{\dot{Q}}}{p'/\rho c^2} = \frac{E_a}{RT_b}\left(\gamma - 1\right)\frac{q-1}{2}\frac{A(\omega)}{B(\omega)}, \tag{2}$$

which represents a model for the transfer function of the flame.

In the above expressions the mass flux fluctuations are normalized by the mass flux of the undisturbed planar flame ρs_l, with s_l the laminar flame speed and the pressure fluctuations by ρc^2, with c the speed of sound. T_b and T_0 stand respectively for burned and fresh gases temperature and E_a is the activation energy. The response is seen to depend on the reduced frequency $\omega\tau_f$, the reduced activation energy $\beta = \frac{E_a}{RT_b}\frac{T_b - T_0}{T_b}$, the isentropic exponent γ and the fuel Lewis number Le.

Independent derivations by McIntosh [12, 13], covering a wider range of frequencies give slightly different expressions for the above quantities. For frequencies of the order of the inverse of the flame transit time $\omega\tau_f = O(1)$ results of the two models are very similar, as shown in [22]. The main differences appear for $\omega\tau_f$ close to 1 for high Lewis numbers [22], and the models are formally identical for Lewis numbers equal to unity.

Wangher et al. [22] presented the first attempt to validate experimentally the analytical models presented above. They measured oscillations of the OH

luminiscence signal obtained when exciting acoustically lean $\phi = 0.625$ planar flames with reduced frequencies ranging from 0.4 to 9. Their measurements showed that the amplitude of fluctuations of OH chemiluminescence intensity is rather constant when varying the frequency of the forcing, for the full frequency domain, and that its level is well above that predicted by the model (see Fig. 5 in the mentioned paper). Their conclusion was that either the OH concentration was not a good measure of the flame response or else the analytical model, derived from a one-step Arrhenius assumption was not adequate, and that a multistep chemistry study would be needed.

We will see in our numerical study that both the fuel consumption rate and the heat release rate fluctuations amplitudes in our simulations have a magnitude and a frequency dependency slightly above the predictions of the model in Eq. (2) while OH production rate fluctuations amplitude grows with frequency, with a dependence similar to that predicted by the mass flux model of Eq. (1).

3 Numerical model formulation

We use numerical experiments to investigate 1-D premixed flames interacting with acoustic waves of characteristic times of similar order and with wavelength much longer than the flame width, as presented in the sketch of Fig. 1. A planar premixed steady methane flame with $\phi = 0.625$ and at 300 K and 1 atm with a flame speed s_l of about 15 cm/s and a width $\delta_f = 1$ mm is first established, on a 1000 points grid corresponding to a 7 mm domain[1]. Acoustic waves are then imposed with an amplitude $p' = 500$ Pa and frequencies ω ranging from 50 Hz to 3000 Hz, corresponding to reduced frequencies $\omega\tau_f$=.33 to 20.

Our study has two main goals. First, we want to compare results obtained with a compressible and an incompressible solver using totally different numerical techniques. Second, we want to validate the Clavin et al. [2] model against our numerical experiments, in which we can use detailed and reduced chemistry, as well as one-step chemistry models.

We use two different numerical models for the computations. The first one is an incompressible zero-Mach-number solver, which uses implicit finite differencing, and for which the pressure waves are represented by time fluctuations of the background pressure $p(t)$. The second is a compressible finite difference solver normally used for direct numerical simulations (DNS) and in which the full acoustics are resolved. To study the sensitivity of results to variations of the complexity of chemistry modelling we try three different approaches. The different numerical tools as well as the different chemistry models are briefly presented in the following.

3.1 The incompressible solver

We solve the variable density zero-Mach-number equations in one spatial dimension on a fixed grid. The balance equations for species mass fractions and

[1]Some compressible calculations, corresponding to smaller frequencies, needed a longer domain to capture the flame position fluctuation: 14 mm over 2000 points

temperature are

$$\rho\frac{\partial Y_s}{\partial t} + \rho u\,\frac{\partial Y_s}{\partial x} = -\frac{\partial j_s}{\partial x} + M_s\,\dot{\omega}_s, \tag{3}$$

$$\rho c_p\frac{\partial T}{\partial t} + \rho u c_p\,\frac{\partial T}{\partial x} = \frac{\mathrm{d}p}{\mathrm{d}t} - \frac{\partial q}{\partial x} - \sum_s j_s\,\frac{\partial h_s}{\partial x} - \sum_s h_s\,M_s\,\dot{\omega}_s, \tag{4}$$

with $s = 1, \ldots, n_s$ and n_s is the number of different species in the system. Here, ρ is the density, Y_s the mass fraction of species s, u the velocity, j_s the species diffusive flux, M_s the molecular weight of species s, $\dot{\omega}_s$ the chemical source term of species s, c_p the heat capacity at constant pressure, p the pressure, q the heat flux, and h_s the enthalpy of species s including the heats of formation. For the equation of state of a mixture of ideal gases we have

$$p = \rho T \sum_s Y_s R_s, \tag{5}$$

with R_s denoting the individual gas constant of species s.

In the zero-Mach-number limit the thermodynamic pressure p is spatially constant. In this case a divergence constraint on the velocity can be derived from the energy equation [9]:

$$\frac{\partial u}{\partial x} = -\frac{1}{\gamma\,p}\frac{\mathrm{d}p}{\mathrm{d}t} + \mathcal{U}, \tag{6}$$

where γ is the ratio of specific heats and $\mathcal{U}$ is given by

$$\mathcal{U} = -\frac{1}{\rho c_p T}\left\{\frac{\partial q}{\partial x} + \sum_s j_s\,\frac{\partial h_s}{\partial x}\right\} - \frac{1}{\rho}\sum_s\left\{\frac{M}{M_s}\frac{\partial j_s}{\partial x}\right\} + \frac{1}{\rho}\sum_s\left\{\frac{M}{M_s} - \frac{h_s}{c_p T}\right\}\dot{\sigma}_s.$$

Here M denotes the mean molecular weight of the mixture and $\dot{\sigma}_s = M_s\,\dot{\omega}_s$. Integrating (6) over the whole domain from $x = x_1$ to $x = x_1 + L$ gives a relation between the global pressure change and inflow and outflow velocities, u_1 and u_2,

$$\frac{\mathrm{d}p}{\mathrm{d}t} = \frac{\gamma\,p}{L}\left\{\int_{x=x_1}^{x_1+L}\mathcal{U}\;\mathrm{d}x - (u_2 - u_1)\right\}. \tag{7}$$

Note, that the acoustic pressure is similar to the thermodynamic pressure only a function of time when the wave length is much larger than the domain considered. This enables us to explicitly prescribe the lhs of (7) via

$$\frac{\mathrm{d}p}{\mathrm{d}t} = A\,\omega\,cos(\omega\,t), \tag{8}$$

where A is the amplitude of the pressure perturbation and $\omega = 2\pi f$ with the frequency f.

The velocity u in eq. (3), (4), and (6) represents the flow velocity induced by dilatational effects due to compression, diffusion, and chemical reactions as given

by (6). The inflow boundary condition u_1 is continuously adapted so as to keep the flame structure in the domain. Note that u_1 can be chosen arbitrarily since the problem is Galilean invariant. The outflow condition u_2 then is uniquely determined using Eq. (7).

The zero-Mach-number equations are solved numerically using standard second-order finite-difference discretization. The time integration of the stiff set of equations is performed using the most recent version of the DAE solver IDA of the SUNDIALS package [7]. Thermodynamic and transport properties as well as reaction rates are calculated using the C++ interface of the CANTERA software package [6].

3.2 The compressible solver

The fully compressible Navier Stokes equations including chemical species equations are solved numerically using 6th order compact finite differences [10] for spatial and 3rd order Runge-Kutta for time integration in a 1-D domain. The time step is given by the minimum between the acoustic CFL condition and the chemical time step of the fastest reaction, which can in principle vary along the simulation. For this flame and resolution it is of the order of 10^{-8}s. The most delicate point in these simulations is the imposition of boundary conditions at the inlet of the domain: we need to impose an acoustic wave entering the domain and at the same time make the inlet non reflecting for possible waves travelling from the interior of the domain towards the inlet. This problem was studied by Kaufmann et al. [8], and they showed that such a condition can not be fulfilled if velocities are imposed at the inlet. Instead, they propose a method, called the inlet wave modulation method (IWM [8]), based on NSCBC [18, 1], in which the amplitude of characteristic waves travelling towards the interior of the domain is imposed. Non reflecting conditions are also imposed at the outlet.

The solver was designed for DNS of reacting turbulent flows and contains thermodynamic and transport libraries as well as routines for the calculation of reaction rates based on the elemental mechanisms [1]. Diffusion velocities are calculated using a mixture-based formulation with variable Lewis numbers for all species.

3.3 The different chemistry models

In this study we use three different chemistry models:

- The well established GRI3.0 mechanism [21], designed to model natural gas combustion provides a very detailed and extensively validated model, containing 53 species and 325 reactions.

- A slightly less complex model using a reduced methane mechanism proposed by Peters [17] and having 16 species including OH. The established mechanism has recently been successfully used for modeling thermoacoustic instabilities and HCCI type combustion [14, 16].

- The simplest model is a classical global one-step irreversible reaction, $CH_4 + 2O_2 -> 2H_2O + CO_2$, with a rate given by an Arrhenius expression. Here we used the Arrhenius parameters proposed in [5] for a lean methane flame.

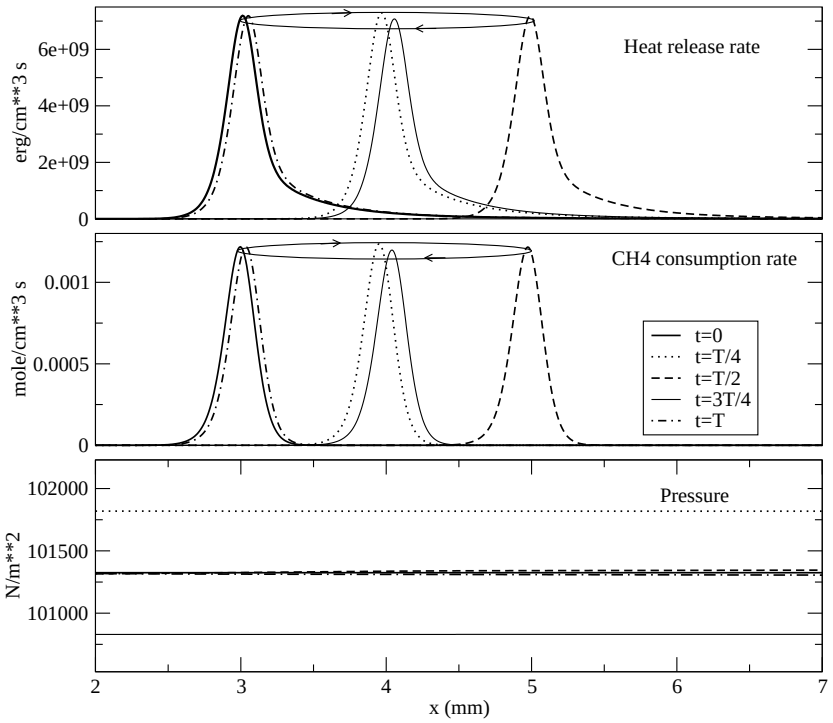

Figure 2: Heat release rate, CH_4 consumption rate and pressure in the computational domain over one cycle for a wave with amplitude $p' = 500$ Pa and frequency $\omega = 500$ Hz ($\omega\tau = 3.3$).

4 Results

4.1 Compressible vs. incompressible results

The first goal was to validate the incompressible versus the compressible approaches. Both codes start from a converged stationary laminar lean ($\phi = 0.625$) methane flame structure. This flame is perturbed by one acoustic mode with an amplitude of 500 Pa and different frequencies: 50, 155, 500, 1000, 1500 and 3000 Hz. While the detailed acoustic wave propagation is solved in the compressible approach, in the incompressible simulations it is represented by a spatially constant pressure varying in time with frequency dependent rate (see Eq. 7). This incompressible approach should be valid in the present conditions since the wavelength is very long compared to the flame width and $Ma \ll 1$.

Fig. 2 presents the evolution of heat release and CH_4 consumption rate over one cycle in the compressible simulation, together with the pressure field in the domain at the same times. In the compressible formulation the acoustic waves are travelling towards the flame and across it, which means that a fraction of the fluctuations are reflected at the flame. Nevertheless, for the long wave lengths of the present study this effect is very small, and it can be seen that pressure is almost spatially constant in the computational domain.

The values of the integral over the computational domain of the heat release rate and the CH_4 consumption rate are extracted along the simulations and

presented as a function of time in Fig. 3 and 4, together with the oscillations of the forcing pressure. The represented pressure variations correspond to the constant-in-space pressure for the incompressible simulations, and to the pressure at the domain inlet (approximately constant in space) for the compressible code results.

It becomes obvious from these figures that the obtained time series for the normalized heat release and fuel consumption rate are nearly identical for the two different numerical approaches. Furthermore, results from the runs using Peters and GRI3.0 mechanisms are very similar, at least for these global quantities. Small phase and amplitude shifts between heat release and fuel consumption rate are observable, showing the multi-step dependence of heat release rate.

4.2 Flame response results and analytical model validation

The second part of the numerical analysis investigates the frequency dependence of heat release, fuel consumption rate and OH production rate fluctuations. The amplitude of the fluctuations of the heat release rate and the fuel consumption rate obtained in the simulations are plotted in Fig. 5 as a function of the reduced frequency $\omega\tau_f$ of the forcing acoustic wave. The amplitude of both heat release and methane consumption rate fluctuations are normalized in these plots with the amplitude of pressure fluctuations measured with ρc^2 as in the expression of Eq. (2). Also included in the plot is the model for $\dot{Q}'$ as given by Eq. (2). To produce the curves corresponding to the model we used typical values of $\beta = 9$ and 10, $Le = 1$, and $T_b = 1710$ K, characteristic of our flames.

We observe that the normalized amplitude of oscillations for both the heat release rate and the mass consumption rate of our simulated flames are similar for incompressible and compressible simulations and for the GRI3.0 and the Peters' chemical schemes. Moreover, they both present a frequency dependence similar to what the model predicts for $\dot{Q}'$, but at a slightly higher amplitude level. Nevertheless, the comparison to the experimental results shown in Fig. 5 from Wangher et al. [22] is quite good.

If we look at the phase results shown in Fig. 6 we see the same tendency, namely that our numerical results agree better with the experimental results (Fig. 7 from Wangher et al. [22]) than with the model predictions. The experiments and the numerical results clearly show a frequency dependent sign change in the phase response, whereas in the model the phase change is always positive. Further the phase shift decay with frequency is slightly more pronounced by the compressible as by the incompressible calculations.

4.3 One step chemistry model

We performed further calculations of the response of a planar premixed flame to acoustic waves of amplitude $p' = 500$ Pa and frequencies ranging from $\omega = 50$ to 3000 Hz using a one step global chemical model with a reaction rate given by the Arrhenius expression:

$$\dot{w} = K[CH_4][O_2]e^{-\frac{E_a}{RT}} \tag{9}$$

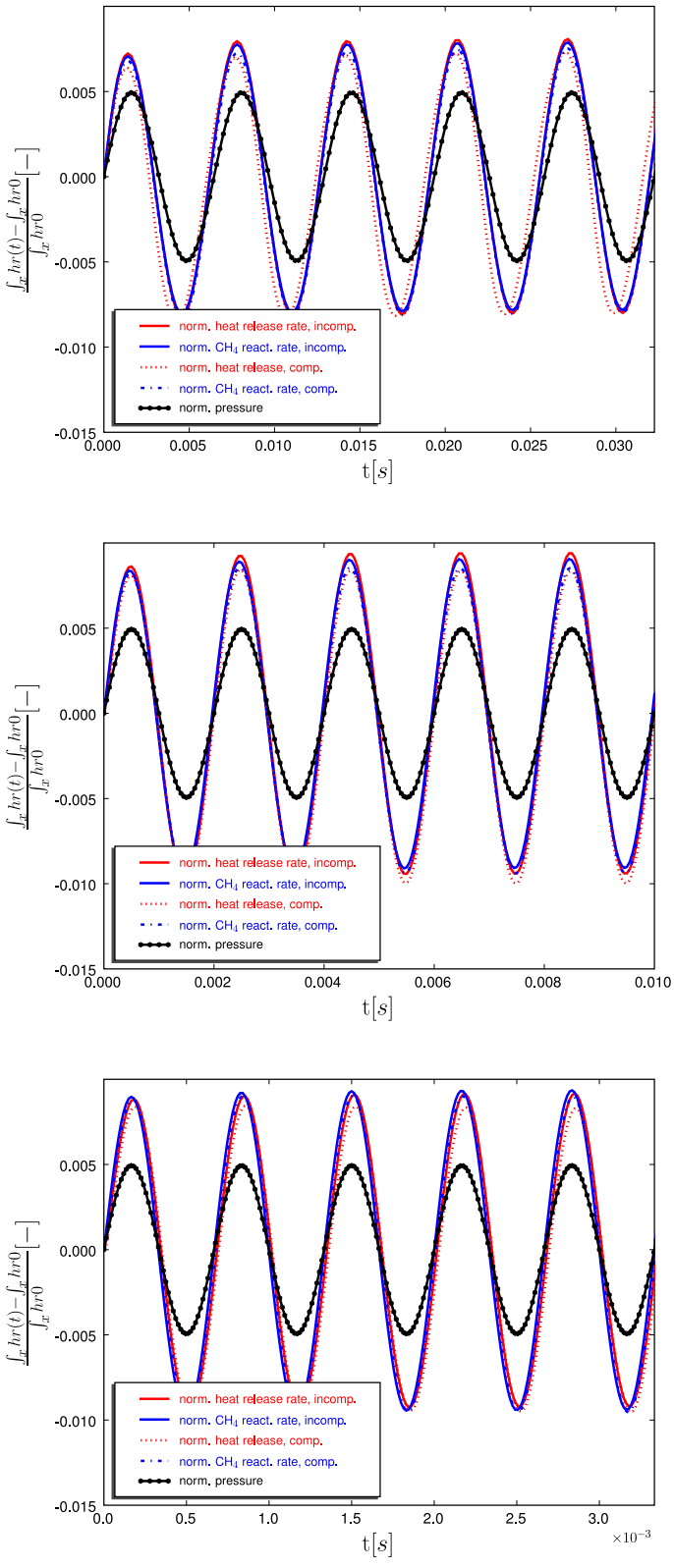

Figure 3: Time series of the normalized heat release, fuel consumption, and pressure during the acoustic perturbation of a laminar methane flame (ϕ = 0.625) with 500 Pa. Results correspond to a perturbation of 500 Pa and 155 Hz, 500 Hz and 1500 Hz, computed with an incompressible and a compressible approach, using the GRI3.0 mechanism.

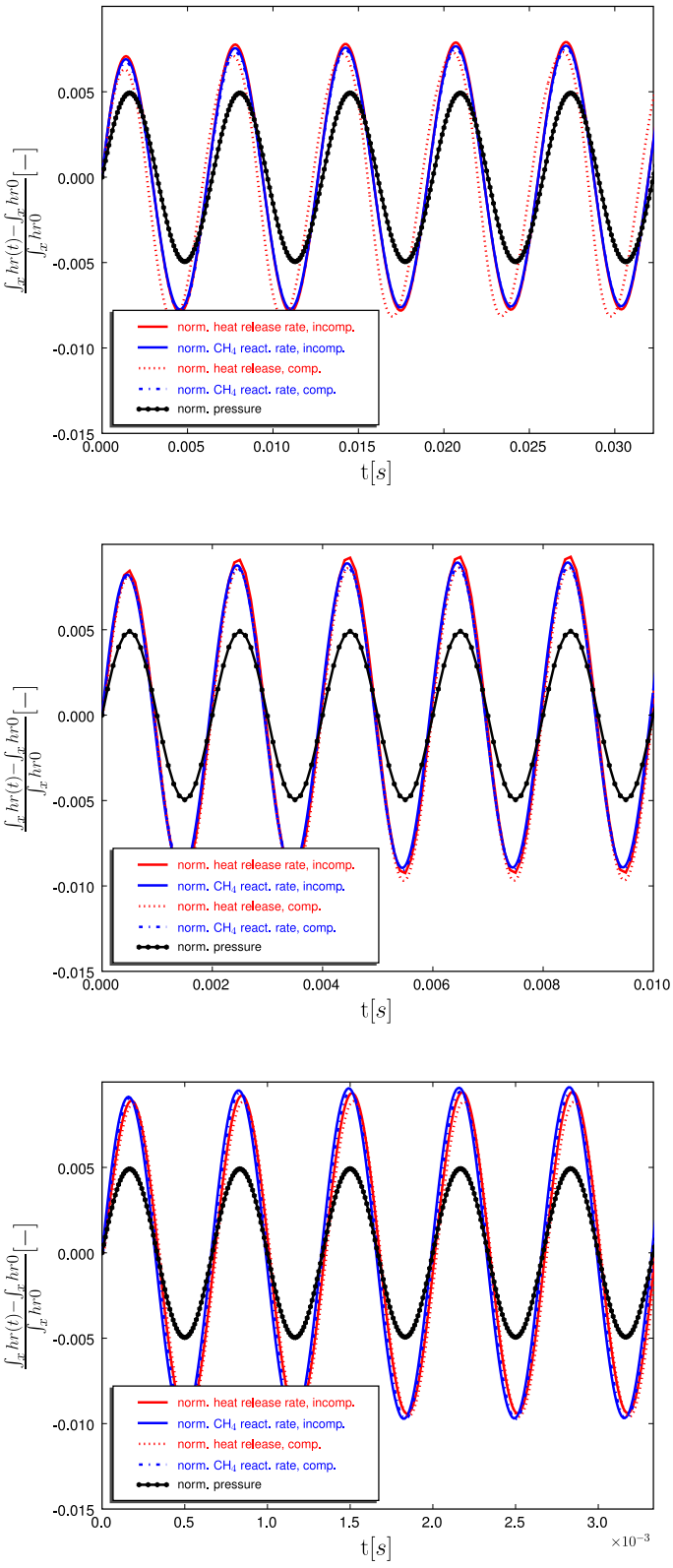

Figure 4: Time series of the normalized heat release, fuel consumption, and pressure during the acoustic perturbation of a laminar methane flame (ϕ = 0.625) with 500 Pa. Results correspond to a perturbation of 500 Pa and 155 Hz, 500 Hz and 1500 Hz, computed with an incompressible and a compressible approach, using the Peters mechanism.

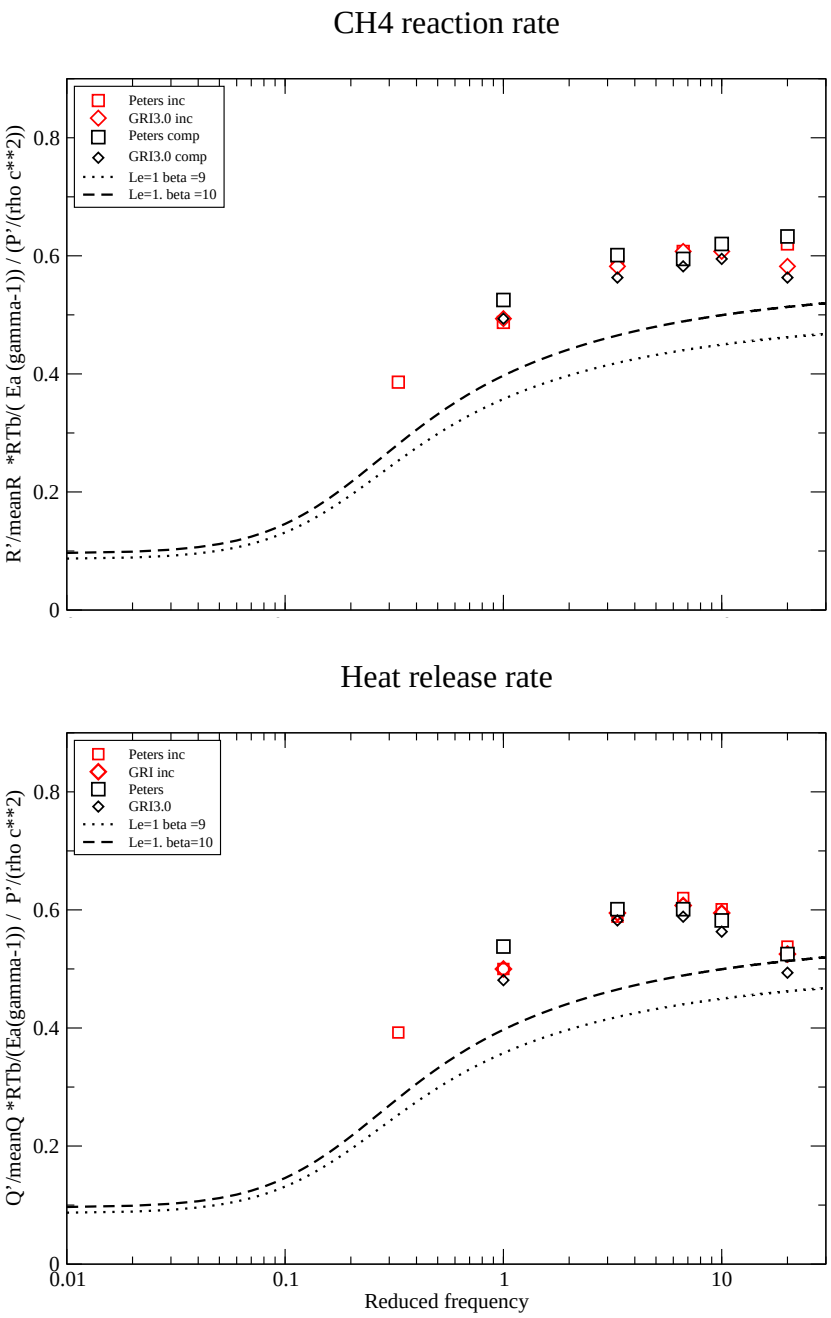

Figure 5: Amplitude of the fuel consumption rate and heat release rate fluctuations divided by the pressure fluctuations' amplitude compared to the model for heat release fluctuations $\dot{Q}'$ from Eq. (2).

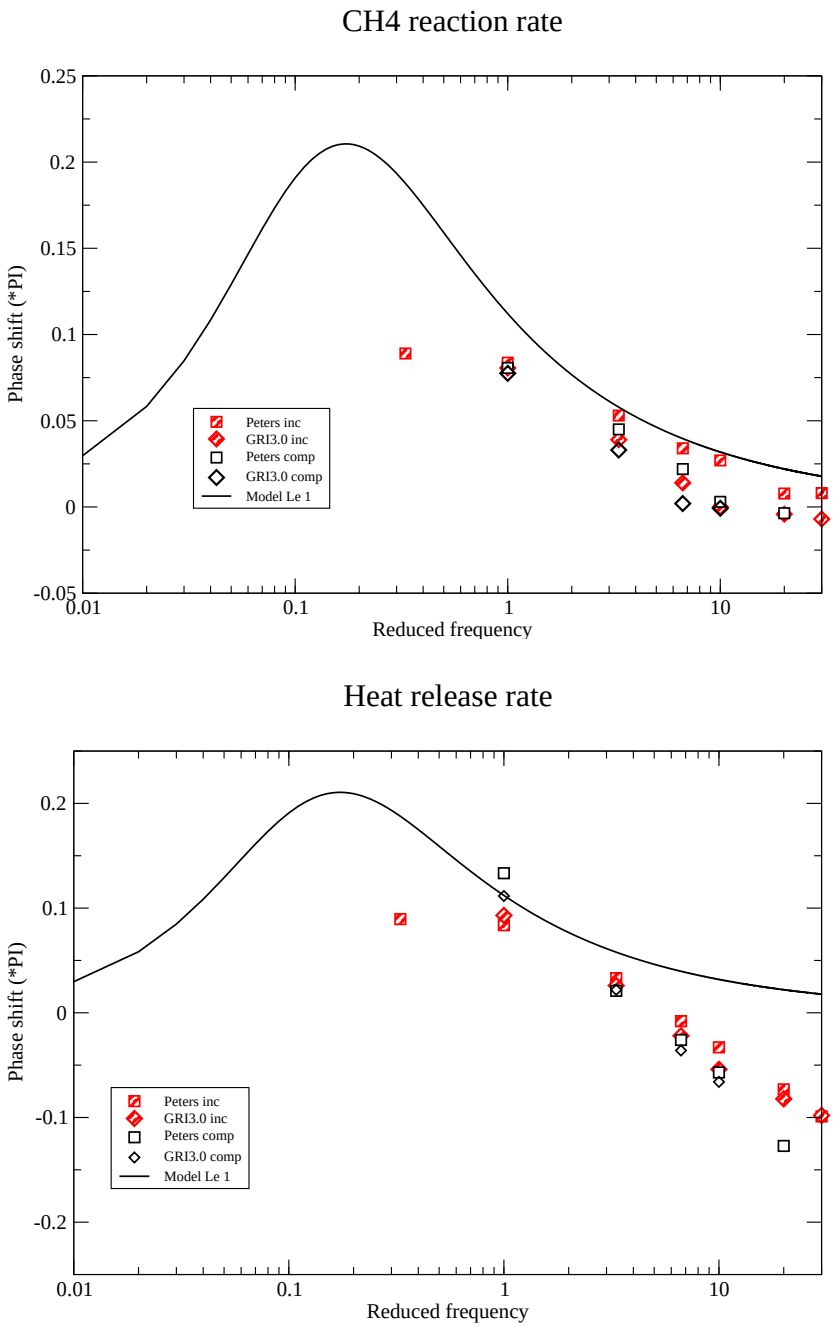

Figure 6: Phase difference for the fuel consumption rate and heat release rate fluctuations when the detailed mechanisms are used.

and reaction constants $K = 6.910^{14}$ and $E_a = 31594.0$ (units: cm, kcal, mole, K), corresponding to the values proposed in [5] for a lean methane flame with $\phi = 0.625$.

Fig. 7 presents the amplitudes of oscillations of the heat release rate and methane consumption rate in the flame for acoustic waves of varying frequencies, as a function of the reduced frequency. Also included are the predictions of the model by Clavin et al. [2] for $Le = 1$.

The one step Arrhenius model appears to behave closely to detailed chemistry mechanism for the lower frequencies, with the amplitude of heat release rate and methane consumption rate increasing with frequency. However, for reduced frequencies from about 8 to 20, the detailed chemistry simulations predict an almost constant amplitude for the response, while the one step model results in a continuous increase in the amplitude. Regarding the phase response in Fig. 8, as the analytic model, the one step model always shows a positive shift, which is not the case for the more detailed mechanisms (see Fig. 6) from the last section and the experimental results.

5 Conclusions

We have presented numerical simulations of the response of a lean methane flame to acoustic waves of frequencies of the order of the flame transit time. As a first objective we have been able to demonstrate the equivalence of an incompressible approach and the compressible approach for this case of a low Mach number flame and long wave length of acoustic perturbations.

The results show the influence of the adopted chemical mechanism on the flame response. For the two multi-step mechanisms the frequency dependence of the heat release fluctuations $\dot{Q}'$ reproduces the tendencies of the models in Clavin et al. [2] and McIntosh works [12, 13] over a wide range of frequencies even if the amplitude is slightly higher. The higher amplitude is also seen in the experiments reported by Wangher et al. [22].

One step mechanisms based on an Arrhenius type rate give similar responses up to reduced frequencies of order 1, and present a tendency to increasing response for higher frequencies. Most probably a different dependency on the concentrations of the reactants and thus on density will be needed to change this high frequency behavior.

The one step results as well as the the analytic model does not predict a sign change in the frequency dependance of the phase response, while the experimental and numerical results using the more complex chemical mechanisms clearly do.

Acknowledgements
This work was partially supported by the Spanish Ministry of Science through project ENE-2008-06515-C04-02 and Madrid's Regional Government through the COMLIMAMS program. Heiko Schmidt gratefully acknowledges fruitful, constructive discussions with M. Oevermann concerning the incompressible code as well as with J. Moeck on flame acoustics.

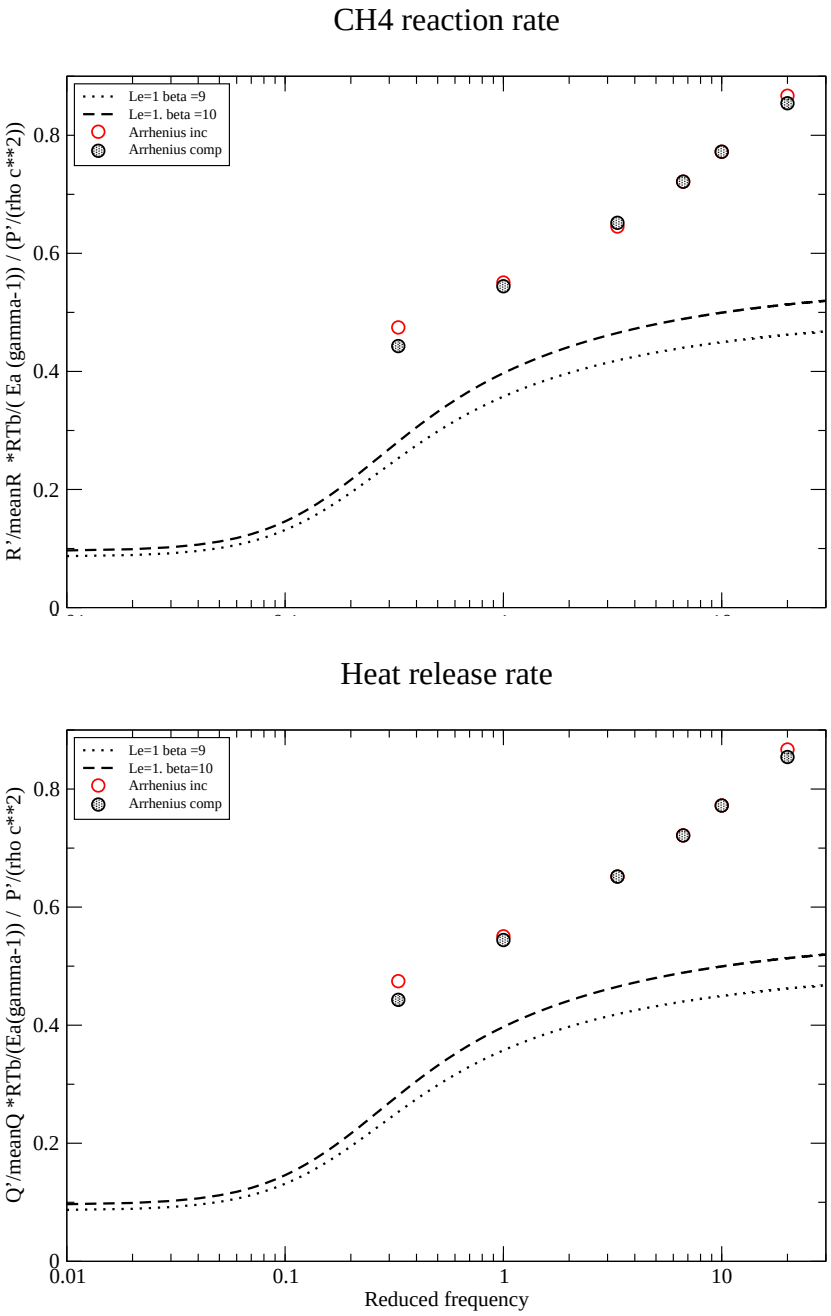

Figure 7: Frequency dependence of the amplitude of the heat release and fuel consumption rate divided by the pressure amplitude for one step chemistry mechanisms

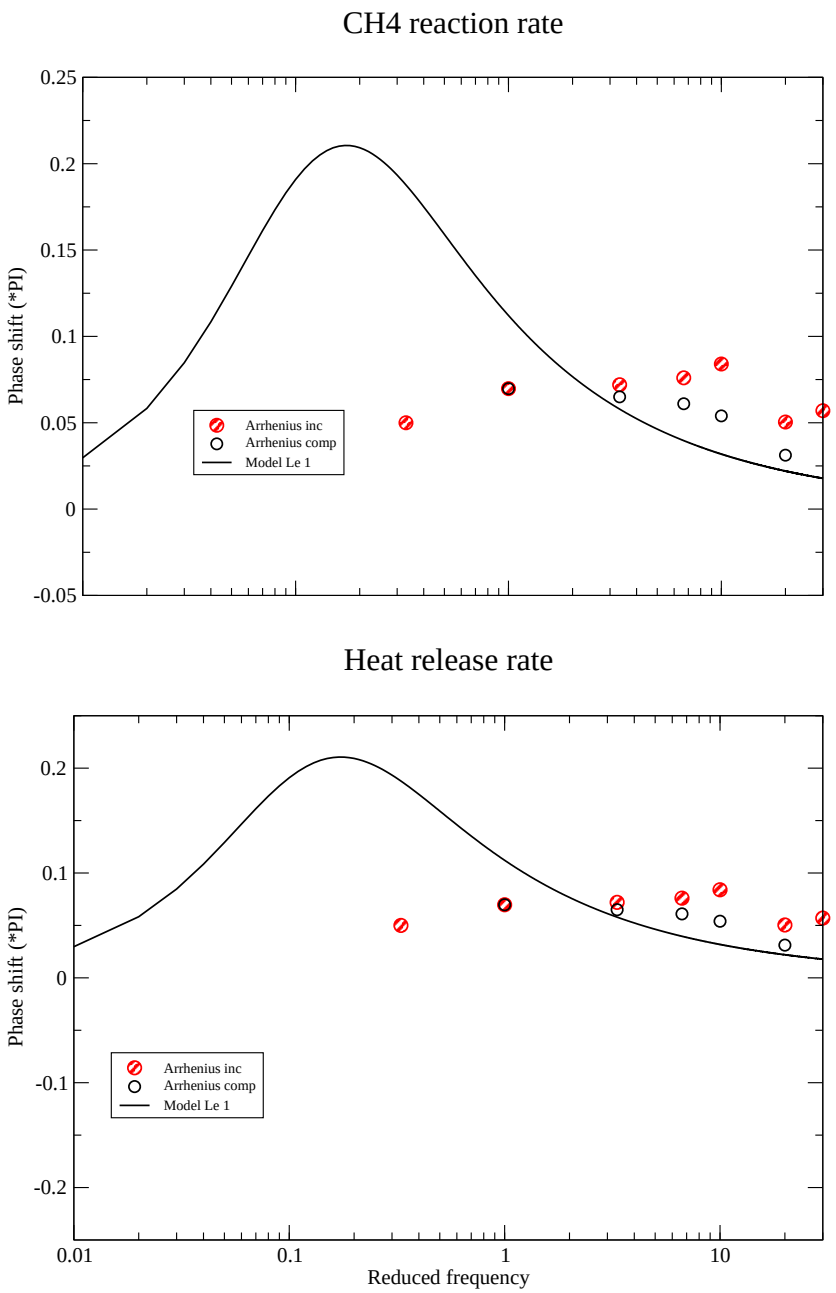

Figure 8: Phase difference for the fuel consumption rate and heat release rate fluctuations when the one step mechanism is used

References

[1] M. Baum, T. Poinsot, and D. Thévenin. Accurate boundary conditions for multicomponent reactive flow. *Journal of Computational Physics*, 116:247–261, 1994.

[2] P. Clavin, P. Peclé, and L. He. One-dimensional vibratory instability of planar flames propagating in tubes. *Journal of Fluid Mechanics*, 216:299–322, 1990.

[3] S. Ducruix, D. Durox, and S. Candel. Theoretical and experimental determination of the transfer function of a laminar premixed flame. *Proc. Combust. Inst.*, 28:765–773, 2000.

[4] D. Durox, F. Baillot, G. Searby, and L. Boyer. On the shape of flames under strong acoustic forcing: a mean flow controlled by an oscillating flow. *Journal of Fluid Mechanics*, 350:295–310, 1997.

[5] E. Fernández-Tarrazo, A. L. Sánchez, A. Liñán, and F. A. Williams. A simple one-stepp chemistry model for partially premixed hydrocarbon combustion. *Combustion and Flame,*, 147:32–38, 2006.

[6] D. Godwin. Cantera: Object-oriented software for reacting flows. http://www.cantera.org.

[7] A. C. Hindmarsh. Sundials: Suite of nonlinear and differential/algebraic equation solvers. Technical report, UCRL-JRNL-200037, Lawrence Livermore National Laboratory, 2004.

[8] A. Kaufmann, F. Nicoud, and T. Poinsot. Flow forcing techniques for numerical simulation of combustion instabilities. *Combustion and Flame*, 13:371–385, 2002.

[9] R. Klein. Semi-implicit extension of a Godunov-type scheme based on low Mach number asymptotics I: one-dimensional flow. *Journal of Computational Physics*, 121:213–237, 1995.

[10] S. Lele. Compact finite difference schemes with spectral-like resolution. *Journal of Computational Physics*, 103:16–42, 1992.

[11] T. Lieuwen and B. T. Zinn. The role of equivalence ratio oscillations in driving combustion instability in low NO_x gas turbines. *Proc. Comb. Inst.*, 27:1809–1816, 1998.

[12] A. C. McIntosh. The linearised response of the mass burning rate of a premixed flame to rapid pressure changes. *Combustion Science and Technology*, 91:329 – 346, 1993.

[13] A.C. McIntosh. Deflagration fronts and compressibility. *Phil. Trans. R. Soc.*, A357:3523–3538, 1999.

[14] J.P. Moeck, M. Oevermann, R. Klein, C.O. Paschereit, and H. Schmidt. A two-way coupling for modeling thermoacoustic instabilities in a flat flame Rijke tube. *Proc. Comb. Inst.*, 32:1199–1207, 2007.

[15] J.P. Moeck, H. Schmidt, M. Oevermann, C.O. Paschereit, and R. Klein. An asymptotically motivated hyrodynamic-acoustic two-way coupling for modeling thermoacoustic instabilities in a Rijke tube. In *Fourteenth International Congress on Sound and Vibration (ICSV14), ISBN 978 0 7334 2516 5, No. 121, 1-9, Cairns, Australia*, 2007.

[16] M. Oevermann, H. Schmidt, and A. R. Kerstein. Investigation of autoignition under thermal stratification using linear-eddy modeling. *Combustion and Flame*, 155:370–379, 2008.

[17] N. Peters. Fifteen lectures on laminar and turbulent combustion. Technical report, Ercoftac Summer School, RWTH Aachen, 1996.

[18] T. Poinsot and S. Lele. Boundary conditions for direct simulations of compressible reacting flows. *Journal of Computational Physics*, 101:104–129, 1992.

[19] T. J. Poinsot, A. C. Trouvé, D. P. Veynante, S. M. Candel, and E. J. Esposito. Vortex-driven acoustically coupled combustion instabilities. *J. Fluid Mech.*, 177:265–292, 1987.

[20] K. C. Shadow and E. Gutmark. Combustion instability related to vortex shedding in dump combusters and their passive control. *Prog. Energy Combust. Sci.*, 18:117–132, 1992.

[21] G. P. Smith, D. M. Golden, M. Frenklach, N. W. Moriarty, B. Eiteneer, M. Goldenberg, C. Th. Bowman, R. K. Hanson, S. Song, W. C. Gardiner, V. V. Lissianski, and Z. Qin. http://www.me.berkeley.edu/gri mech/. Technical report.

[22] A. Wangher, G. Searby, and J. Quinard. Experimental investigation of the unsteady pressure response of premixed flame fronts to acoustic pressure waves. *Combustion and Flame*, 154:310–318, 2008.

[23] X. Wu, M. Wang, P. Moin, and N. Peters. Combustion instability due to nonlinear interaction between sound and flame. *J. Fluid Mech.*, 497:23–53, 2003.

[24] K. H. Yu, A. Trouvé, and J. W. Daily. Low-frequency pressure oscillations in a model ramjet combustor. *J. Fluid Mech.*, 232:47–72, 1991.